Resonance Raman and EPR Investigations of the D251N Oxycytochrome $P450_{cam}$/Putidaredoxin Complex†

Theodore Sjodin,‡ James F. Christian,‡ Iain D. G. Macdonald,§ Roman Davydov,|| Masashi Unno,‡ Stephen G. Sligar,§ Brian M. Hoffman,|| and Paul M. Champion*,‡

Department of Physics and Center for Interdisciplinary Research on Complex Systems, Northeastern University, Boston, Massachusetts 02115, Departments of Biochemistry and Chemistry and Beckman Institute for Advanced Science and Technology, University of Illinois at Urbana−Champaign, Urbana, Illinois 61801, and Department of Chemistry, Northwestern University, Evanston, Illinois 60201

Received October 31, 2000

ABSTRACT: We have performed resonance Raman and electron paramagnetic resonance (EPR) studies on the dioxygen bound state of the D251N mutant of cytochrome $P450_{cam}$ (oxy-$P450_{cam}$) and its complex with reduced putidaredoxin (Pd). The D251N oxy-$P450_{cam}$/Pd complex has a perturbed proton delivery mechanism and shows a significantly red-shifted UV−visible spectrum as observed in Benson et al. [Benson, D. E., Suslick, K. S., and Sligar, S. G. (1997**)** *Biochemistry 36,* 5104−5107]. The red shift has been interpreted to indicate a major perturbation of the electronic structure of the oxy-heme complex. However, we find no evidence that electron transfer has occurred from Pd to the heme active site of D251N oxy-$P450_{cam}$. This suggests that both electron and proton transfer are perturbed by the D251N mutation and that these processes may be coupled. Three oxygen isotope sensitive Raman features are identified in the Pd complex, and occur at 1137, 536, and 399 cm^{-1}. These values are not significantly different from those for WT or D251N oxy-$P450_{cam}$. However, a careful examination of the oxygen stretching feature near 1137 cm^{-1} reveals the presence of three peaks at 1131, 1138, and 1146 cm^{-1}, which we attribute to the presence of conformational substates in oxy-$P450_{cam}$. A significant change in the conformational substate population is observed for the D251N oxy-$P450_{cam}$ when the Pd complex is formed. We suggest that the conformational population redistribution of oxy-$P450_{cam}$, along with the red-shifted electronic spectra, reflects a structural equilibrium of the oxy-heme that is perturbed upon Pd binding. We propose that this structural perturbation is connected to the effector function of Pd and may involve changes in the electron donation properties of the thiolate ligand.

Cytochromes P450 comprise a family of heme-containing monooxygenases involved in a variety of oxidative metabolic reactions. The bacterial cytochrome $P450_{cam}$ ($P450_{cam}$)[1] from *Pseudomonas putida* (CYP101) has been the most systematically investigated as a model for the entire family of cytochrome P450 enzymes (*1*). Unlike other heme proteins, such as myoglobin and hemoglobin, $P450_{cam}$ uses the thiolate of Cys357 as the proximal ligand of the heme iron and possesses a hydrophobic distal heme pocket where a substrate, *d*-camphor, is bound. $P450_{cam}$ catalyzes the stereospecific hydroxylation of the substrate to form 5-*exo*-hydroxycamphor by adding an oxygen atom to the camphor substrate.

The $P450_{cam}$ catalysis reaction requires an external source of two electrons from NADH through the combined action of the FAD−flavoprotein putidaredoxin reductase and the iron−sulfur (2Fe-2S) protein putidaredoxin (Pd). It has been determined from kinetic and fluorescence studies that formation of a complex between Pd and $P450_{cam}$ is required for product formation (*2*, *3*), and that Pd has an effector role in product formation, in addition to its role in electron transfer (*3*, *4*). In the reaction cycle, Pd donates an electron to ferric camphor-bound $P450_{cam}$ (**2**) (throughout the text, boldface numbers refer to species in Scheme 1), forming the high-spin ferrous state (**3**). Dioxygen then binds to the heme iron to form the oxy-$P450_{cam}$ (**4**), and a second one-electron reduction takes place, which is followed by rapid product formation. The rapid product formation impedes the spectroscopic observation of intermediates **5**−**7** in the wild-type Pd reconstituted system at room temperature. The oxy-$P450_{cam}$ intermediate **4** readily forms in the absence of Pd, but it autoxidizes to form the ferric substrate-bound $P450_{cam}$ **1** without product formation. The study of **4** is difficult because the autoxidation process limits its lifetime to about 10 min at 4 °C in solution at pH 7 (*5*). This makes spectroscopic characterization quite formidable (*6*, *7*).

There have been a number of different strategies used to stabilize the reactive intermediates to allow their study. One technique is to use cryogenic temperatures to slow the autoxidation rate of **4** in the absence of Pd. This approach has been used to determine the resonance Raman spectra of **4** (*7*, *8*), and very recently the X-ray crystallographic structure

† This work was supported by NIH Grants DK-35090 (P.M.C.), GM-31756 (S.G.S.), GM-33775 (S.G.S.), and HL-13531 (B.M.H.) and by NSF Grant MCB-9904516 (P.M.C.).

* To whom correspondence should be addressed. Tel.: 617-373-2918, Fax: 617-373-2943, E-Mail: champ@neu.edu.

‡ Northeastern University.

§ University of Illinois at Urbana−Champaign.

|| Northwestern University.

[1] Abbreviations: $P450_{cam}$, cytochrome $P450_{cam}$; oxy-$P450_{cam}$, ferrous dioxygen bound cytochrome $P450_{cam}$; Pd, putidaredoxin; RR, resonance Raman; KSIE, kinetic solvent isotope effect.

10.1021/bi002510b CCC: $20.00
Published on Web 05/18/2001

Scheme 1

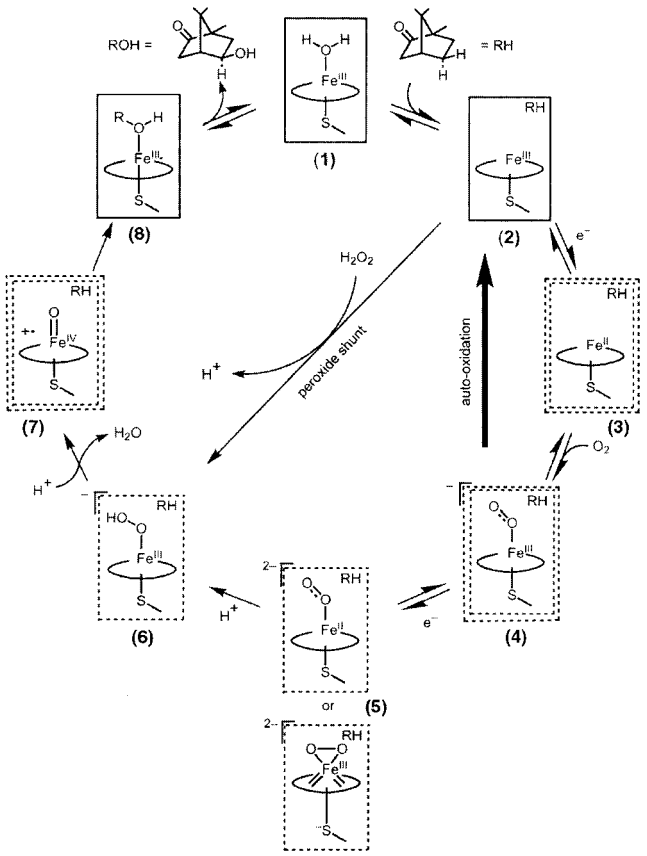

of **4** (*9*). One can isolate other intermediates by using electrons produced by the X-ray radiolysis of water to reduce **4** and trap intermediates at cryogenic temperatures. This technique was used to isolate intermediates **5** and **6** for study using electron paramagnetic resonance (EPR) (*10*), and intermediate **7** for the determination of the X-ray crystallographic structure (*9*). At this time, it is not clear whether the reaction pathway using the electrons from X-ray radiolysis is the same as using the physiological electron donor and effector Pd, but it does lead to product formation (*10*).

The first electron reduction (from **2** to **3**) can be carried out by chemical and photochemical reducing agents such as dithionite and proflavin/EDTA. The second electron reduction (from **4** to **5**) can only be accomplished by the use of specific effector molecules (*3*, *4*) or the use of X-ray radiolysis. The role of Pd is unique. For example, iron−sulfur proteins such as spinach ferredoxin and bovine adredoxin can donate the first electron but not the second electron, whereas reduced rubredoxin and cytochrome b_5 can donate the second electron but not the first (*3*).

It is clear that elucidating the structure−function relationships in P450$_{cam}$ requires an understanding of the crucial interactions between P450$_{cam}$ and Pd. Indeed, the electron-transfer reaction between P450$_{cam}$ and Pd has been extensively characterized. In addition to the role of an electron donor to P450$_{cam}$, Pd has been shown to perturb the heme active site of the enzyme (*11*−*15*). For instance, Lipscomb (*11*) performed an EPR study of the P450$_{cam}$/Pd complex at cryogenic temperature and found that the complex formation shifts the spin-state equilibrium of ferric P450$_{cam}$ from the high-spin to the low-spin state. Recently a resonance Raman spectroscopic investigation demonstrated a Pd-induced spin-state change at room temperature (*14*). Makino et al. (*12*) and Unno et al. (*16*) reported that the Fe−CO and C−O stretching frequencies changed when Pd was bound to ferrous CO-P450$_{cam}$, and recent work has also shown significant perturbations to Fe−NO stretching frequencies upon Pd binding to ferrous NO-P450$_{cam}$ (*16*).

Resonance Raman (RR) spectroscopic characterization of the ferric P450$_{cam}$/oxidized Pd complex further reveals that the diprotein complex formation affects the stretching frequency of the heme iron-proximal Cys357 (Fe−S) bond (*14*). The perturbation of the Fe−S bond is in accord with the fact that Pd binds to the proximal surface of P450$_{cam}$ (*17*−*22*).

As discussed above, previous spectroscopic studies indicate that complex formation affects the heme active site of P450$_{cam}$. In addition to these spectroscopically observable effects, Pd provides a necessary effector function that couples the flow of reducing equivalents to successfully turn over substrate in P450$_{cam}$ catalysis (*3*, *4*). Therefore, the Pd binding effect observed spectroscopically may have a functional significance in the P450$_{cam}$ reaction.

In this paper, we investigate the D251N (Asp251 to Asn) mutant of P450$_{cam}$ and use resonance Raman spectra to characterize the oxygenated intermediate at 4 °C in both the presence and absence of Pd. This mutant has been shown to slow the turnover rate (*23*, *24*) and perturb the proton delivery mechanism needed for product formation. In the presence of Pd, a red-shifted absorption spectrum was observed for the oxygenated complex (*23*), suggesting that the second electron might be transferred to the oxygenated intermediate, allowing for the spectroscopic characterization of **5**. However, in this work, we find no evidence from either resonance Raman or EPR spectroscopy for the creation of a peroxy intermediate or for the transfer of a second electron to the heme. The perturbation of *both* electron and proton transfer in the Pd-bound oxygenated D251N mutant suggests that these two processes may be coupled. We also find that Pd binding alters the protein conformational substate populations of the oxygenated complex, which signal changes in the thiolate−iron−oxygen bonds that may be related to the effector function of Pd.

EXPERIMENTAL PROCEDURES

Sample Preparation. Site-directed mutagenesis of the P450$_{cam}$ gene was carried out as described previously (*24*). Wild-type and mutant (D251N) P450$_{cam}$ and native Pd were expressed in *E. coli* and purified using a published procedure (*25*). Protein stocks were flash-frozen and stored at −80 °C (P450$_{cam}$) or in liquid nitrogen (Pd). Purified camphor-bound P450$_{cam}$ preparations with an R_z (A_{392}/A_{280}) ≥1.6 were used for the RR experiments. Purified Pd with A_{325}/A_{280} ≥0.6 was suitable for all RR experiments. The molar ratio of these physiological components is important for quantitative conversion of substrate (*d*-camphor) to product (5-*exo*-hydroxycamphor). It is reported that the minimum molar ratio required for 99% conversion to product is 2.1 Pd:D251N P450$_{cam}$ (*23*).

A 2.1 molar equivalent mixture of oxidized Pd and P450$_{cam}$ was placed in an anaerobic chamber (Coy Products) containing a high-purity nitrogen atmosphere with 5−10% hydrogen and a palladium catalyst. This protein mixture was added to

a 10 molar excess of reductant, sodium dithionite, and eluted rapidly over a preequilibrated 5 mL medium-grade G25 Sephadex column. Equilibration and elution conditions were 50 mM potassium phosphate, pH 8.0, 1.6 mM *d*-camphor. All salts and column materials were purchased from Sigma (St. Louis, MO) in high purity (typically >99%) and used as supplied. Protein samples were eluted and concentrated to ~200 μM P450$_{cam}$ (~420 μM Pd). Aliquots (80 μL) of this reduced mixture were flash-frozen and sealed anaerobically and stored at −80 °C until required for oxygenation. Oxygenation was provided by addition of 5 mL of the appropriate isotopic gas to these sealed vessels followed by rapid transfer to the Raman scattering cell.

Spectroscopic Measurements. A liquid nitrogen cooled CCD detector (Princeton Instruments, Inc.) recorded the Raman spectra after a holographic notch filter (Kaiser Optical Systems, Inc.) removed the excitation light, and a Spex 1870B spectrometer (1200 or 2400 grating, 0.5 m focal length) dispersed the scattered light. The 356.4 and 413.1 nm lines from a krypton ion laser (Coherent Innova 300) excited the samples at a 90° angle, relative to the axis of the collection optics. All the spectra were taken at 4 °C. A quartz spinning cell minimizes the population of photodissociated species and their contribution to the recorded Raman spectrum. A commercial derivative filter software routine (Princeton Instruments, Inc.) eliminated the noise spikes in the spectra, caused by cosmic rays. All Raman spectra were calibrated using neat fenchone. The accuracy of the absolute frequencies is about ± 1 cm^{-1}, and less than ± 0.2 cm^{-1} for relative shifts of strong and/or isolated bands. We determine the peak positions in the Raman spectra by fitting the data with Lorentzian or Voigt functions on a linear background using a nonlinear least-squares fitting routine (Origin PFM, Microcal, Inc.). UV−visible absorption spectra were recorded with a Hitachi U-3410 spectrophotometer.

EPR Measurements. The 35 GHz CW EPR spectra were recorded with a spectrometer of local design that employs 100 kHz field modulation. A detailed experimental description appears in Werst, Davoust, and Hoffmann (*26*). The samples used in the EPR experiments contained 2.1 molar equivalent mixtures of P450$_{cam}$ and Pd, in 0.1 M potassium phosphate buffer (pH 8.0) with 1.6 mM camphor, and 15% v/v glycerol. The anaerobically purified mixture was combined with oxygen under conditions previously described (*23*) and flash-frozen in liquid nitrogen. The EPR sample conditions and protocols are analogous to those discussed in Davydov et al. (*10*) and Benson et al. (*23*).

RESULTS

Figure 1 shows the time dependence of the resonance Raman and UV−visible absorption spectra of WT oxy-P450$_{cam}$ and of the D251N oxy-P450$_{cam}$ complex with Pd. Figure 1A demonstrates the oxidation of oxy-P450$_{cam}$ to its ferric state. The oxidation process is believed to have components due to both auto- and photo-oxidation. These spectra were taken at 4 °C, and at pH 8. Low temperature and high pH lowers the autoxidation rate, allowing for efficient acquisition of the oxy-P450$_{cam}$ Raman spectra. We find that the Soret (near 420 nm) and Q (near 550 nm) absorption bands of the Pd complex show a red shift of several nanometers compared to D251N oxy-P450$_{cam}$ (which has an absorption spectrum that is identical to that of the WT shown in Figure 1A). The red-shifted spectra for the D251N oxy-P450$_{cam}$/Pd complex were first observed by Gerber and Sligar (*24*), and by Benson, Suslick, and Sligar (*23*). In the RR spectra, the most dramatic effect is the clear appearance of two ν_{O-O} modes, which will be discussed in detail later. This figure also demonstrates the oxidation of D251N oxy-P450$_{cam}$ to its ferric state in the presence of Pd. The oxidation rate under these conditions is very similar to what is observed for WT oxy-P450$_{cam}$ without Pd (see Figure 1A).

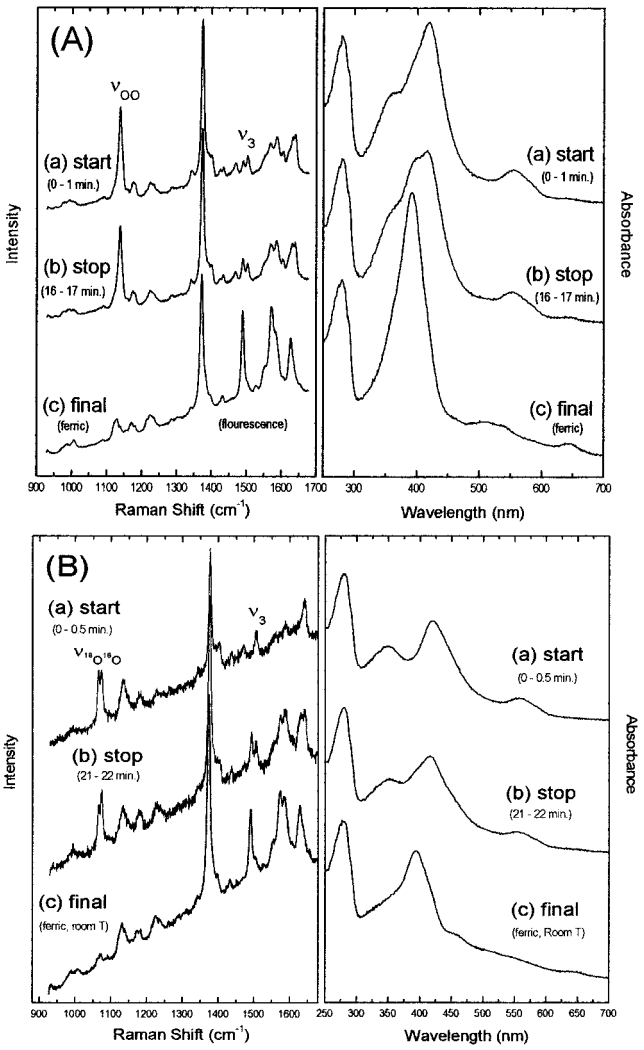

FIGURE 1: (A) Time dependence of resonance Raman and optical absorption spectra of the WT oxy-P450$_{cam}$ at (a) 0−1 min, (b) 16−17 min, and (c) after complete oxidation. The spectra were taken at 4 °C. The Raman spectra were obtained with 413 nm excitation. (B) Time dependence of resonance Raman and optical absorption spectra of the D251N mutant oxy-P450$_{cam}$/Pd complex at (a) 0−0.5 min, (b) 21−22 min, and (c) after complete oxidation. Spectra a and b were taken at 4 °C, and spectrum c was taken at room temperature. The Raman spectra were obtained with 413 nm excitation.

The oxy-P450$_{cam}$ resonance Raman spectrum is characterized by a strong band at 1138 cm^{-1} representing the O−O stretch (*7*, *8*). Figure 2 displays the RR data for $^{16}O_2$ (a and d) and $^{18}O_2$ (b and e), and the normalized difference spectra ($^{16}O_2 - {}^{18}O_2$) for WT oxy-P450$_{cam}$ at 356 and 413 nm excitation. Inspection of the $^{16}O_2 - {}^{18}O_2$ difference spectra at 356 and 413 nm excitation clearly indicates three differ-

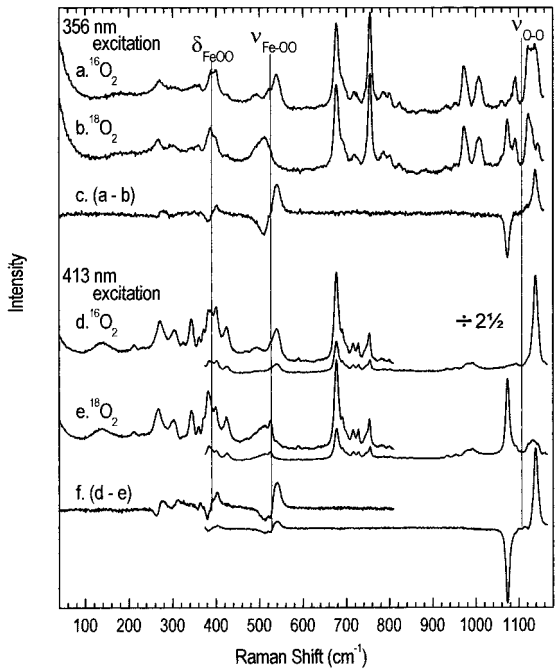

FIGURE 2: Shifts induced due to isotopic labeling of O_2 in WT oxy-P450$_{cam}$ at resonance excitations of 356 nm (a−c) and 413 nm (d−f).

Table 1: O_2-Sensitive Vibrational Frequencies in Oxy-P450$_{cam}$

		WT oxy-P450$_{cam}$ (cm^{-1})		D251N oxy-P450$_{cam}$ (cm^{-1})		D251N oxy-P450$_{cam}$/Pd (cm^{-1})	
		ν_a[a]	ν_b	ν_a	ν_b	ν_a	ν_b
ν_{O-O}	$^{16}O_2$	1131	1138	1128	1136	1129	1137
	$^{18}O_2$	1066	1073	1061	1070	1062	1071
ν_{Fe-OO}	$^{16}O_2$	—[b]	540	—[b]	536	521	536
	$^{18}O_2$	—[b]	510	—[b]	505	487	505
δ_{FeOO}	$^{16}O_2$		401		399		∼399
	$^{18}O_2$		383		383		∼381

[a] ν_a and ν_b refer to the two conformations associated with the major ν_{O-O} and ν_{Fe-OO} stretching vibrations. [b] Too weak to be observed.

ence signals which have been assigned to FeOO bending (δ_{FeOO}), Fe−OO stretching (ν_{Fe-OO}), and O−O stretching (ν_{O-O}) vibrations (*7*, *8*, *27*). The ν_{O-O} mode shows a large resonance enhancement over the δ_{FeOO} and ν_{Fe-OO} modes at 413 nm excitation compared to 356 nm excitation. Another feature, which is also sensitive to the isotopic labeling of the oxygen, appears at 290 cm^{-1} and has not yet been categorically assigned. The frequencies of the assigned oxygen-sensitive modes appear in Table 1.

Figure 3 compares the high-frequency RR spectra of the D251N mutant oxy-P450$_{cam}$/Pd complex to WT and D251N mutant oxy-P450$_{cam}$. The D251N mutation has a negligible perturbation on the frequency and enhancement of the core size marker bands. Upon complex formation with Pd, there is no observed shift in the oxidation marker band, ν_4, and small shifts, if any, in the core size marker bands. The clear appearance of multiple components of the O_2 stretching band represents the largest Pd-induced perturbation in the spectra. The components can be seen in detail in Figure 4 where the WT, D251N, and D251N/Pd ($^{16}O_2 - {}^{18}O_2$) difference spectra are displayed at the ν_{O-O} band frequency. The spectral profile of the D251N/Pd complex clearly shows two major components within the ν_{O-O} band. To quantify these components,

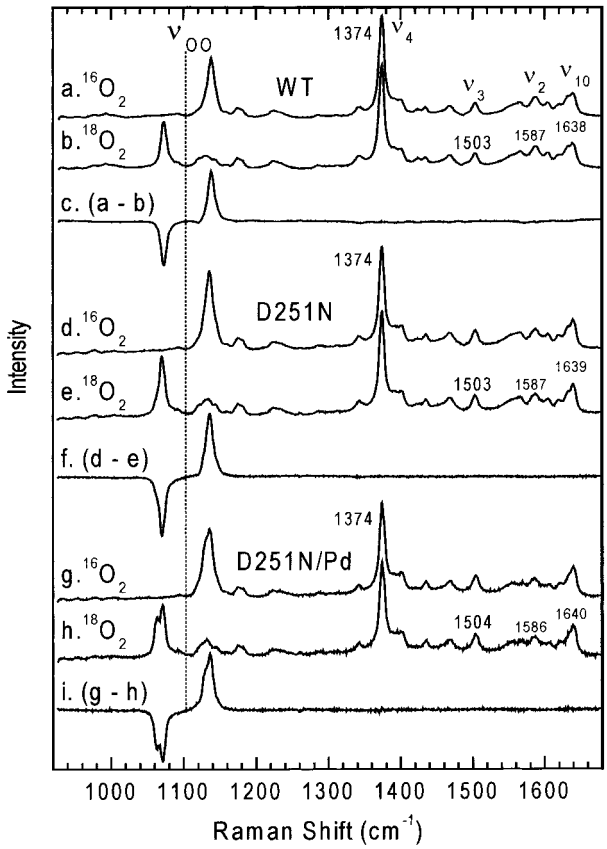

FIGURE 3: "Core-size" marker peaks and shifts induced due to isotopic labeling of O_2 on WT (a−c), D251N (d−f), and D251N/Pd (g−i).

the difference spectra were fit to multiple Voigt profiles. Each spectrum was fit and analyzed independently. The best fits to the WT and D251N samples contained three peaks. The relative positions and amplitudes of the minor peaks with respect to the major peaks were nearly identical for both the $^{16}O_2$ and $^{18}O_2$ isotopes. If the origin of the multiple peaks were solely due to coupling to an underlying porphyrin mode (e.g., Fermi resonance), there should be a dramatic difference in the amplitudes and relative peak positions upon O_2 isotopic substitution. Since the relative amplitude and relative peak positions remain fixed, the multiple peaks are assigned as different conformational substates. The ν_{O-O} region of the D251N/Pd complex is fit well using only the two lower frequency components of the uncomplexed protein without Pd, suggesting that Pd binding induces a redistribution of the conformational populations.

Figures 5 and 6 show the low-frequency RR spectra of D251N oxy-P450$_{cam}$ and its Pd complex, along with the $^{16}O_2 - {}^{18}O_2$ difference spectra at 356 and 413 nm excitation, respectively. At 356 nm excitation, the ν_{Fe-OO} mode is clearly broader in the D251N/Pd complex than the D251N mutant (see Figure 5). The data are fit by including a second mode at lower frequency (∼525 cm^{-1}) of roughly equal intensity and width to the ν_{Fe-OO} mode at ∼540 cm^{-1} for the uncomplexed protein. The broadening of ν_{Fe-OO} is consistent with the appearance of multiple components in the ν_{O-O} mode. For 413 nm excitation, the effects of Pd binding on the ν_{Fe-OO} and δ_{FeOO} modes are more complex, due to spectral congestion and the apparent coupling of these modes to underlying porphyrin vibrations.

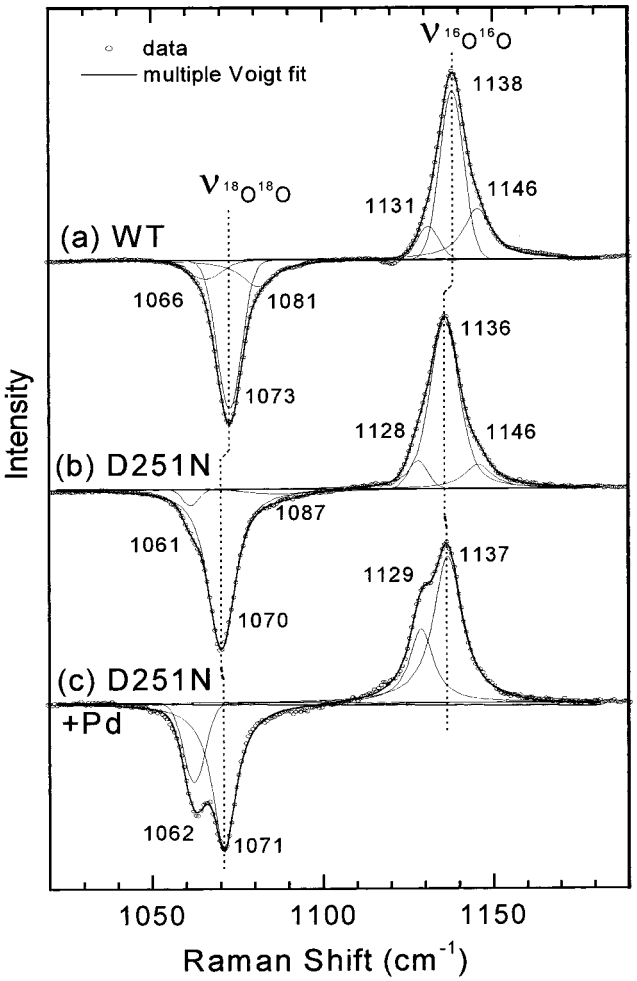

FIGURE 4: Comparison and peak fitting analysis of the O_2 vibration of (a) WT, (b) D251N, and (c) D251N/Pd complex. The solid lines represent fits to three independent Voigt profiles.

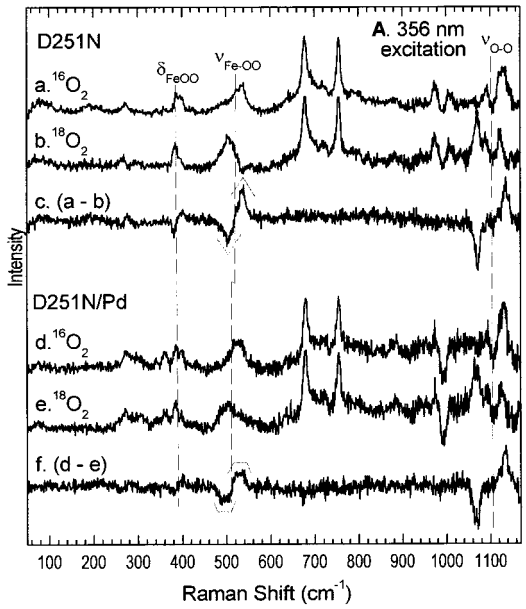

FIGURE 5: Shifts induced due to isotopic labeling of O_2 in (a−c) D251N oxy-P450$_{cam}$ and (d−f) D251N/Pd oxy-P450$_{cam}$ complex. The Raman spectra were obtained with 356 nm excitation.

Figure 7 shows the time dependence of the ν_{O-O} peak areas due to the oxidation (photoinduced and autoxidation) of the sample, using the $^{18}O_2$ isotope to shift the O_2 modes into an uncongested region of the spectrum. This provides information on the relative oxidation rate of the different conformations in the D251N oxy-P450$_{cam}$ and D251N/Pd complex. There is no significant change in the oxidation rate of the dominant conformation at 1061 cm^{-1} upon Pd binding. The measured half-lives for the D251N oxy-P450$_{cam}$ and D251N oxy-P450$_{cam}$/Pd complexes are 29 ± 5 and 26 ± 5 min, respectively. Both the D251N oxy-P450$_{cam}$ and D251N oxy-P450$_{cam}$/Pd complexes exhibit similar oxidation rates for the two conformations, as indicated in Figure 7(c), where the ratios of the peak areas of the two conformations are shown.

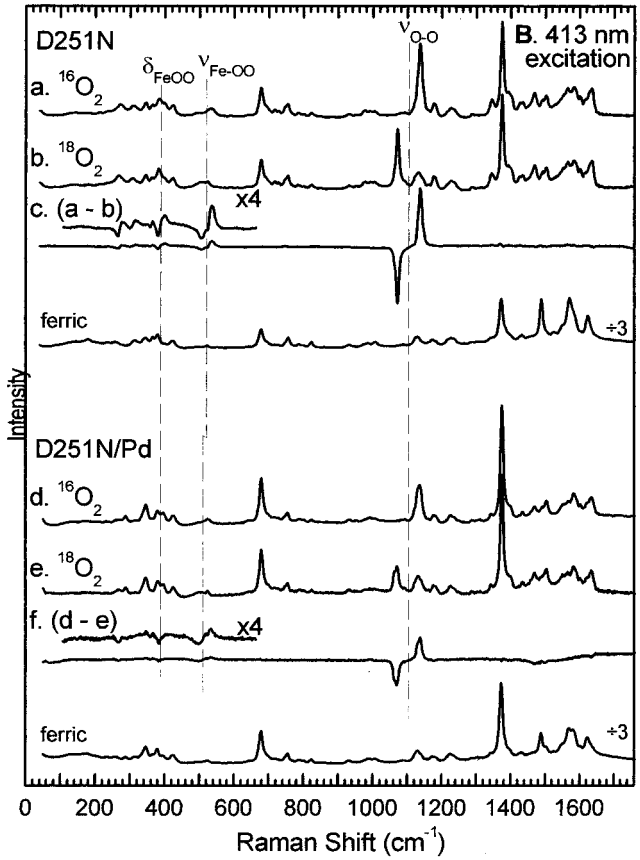

FIGURE 6: Shifts induced due to isotopic labeling of O_2 in (a−c) D251N oxy-P450$_{cam}$ and (d−f) D251N/Pd oxy-P450$_{cam}$ complex The Raman spectra were obtained with 413 nm excitation.

Figure 8 presents the 2 K Q-band EPR spectra of D251N/Pd oxy-P450$_{cam}$. The spectrum of Pd, with $g = (2.02, 1.93)$, indicates reduced Pd is present. This spectrum is identical to that observed by Shimada et al. (*28*), which shows a perturbation of the putidaredoxin structure upon binding to P450$_{cam}$. There is also a very small component of the spectrum with *g*-values characteristic of trace amounts of high- and low-spin ferric P450$_{cam}$ (*29*) present in the sample, due to autoxidation of the ferrous oxy-P450$_{cam}$. There is no indication from the EPR spectra that an electron has transferred from the Pd to the oxy-heme site.

DISCUSSION

Since the discovery that the D251N mutation in P450$_{cam}$ slows the turnover rate for camphor hydroxylation by 1−2 orders of magnitude compared with native P450$_{cam}$ (*24, 30*), there has been hope that the two-electron-reduced oxy complex of this mutant would lead to the spectroscopic

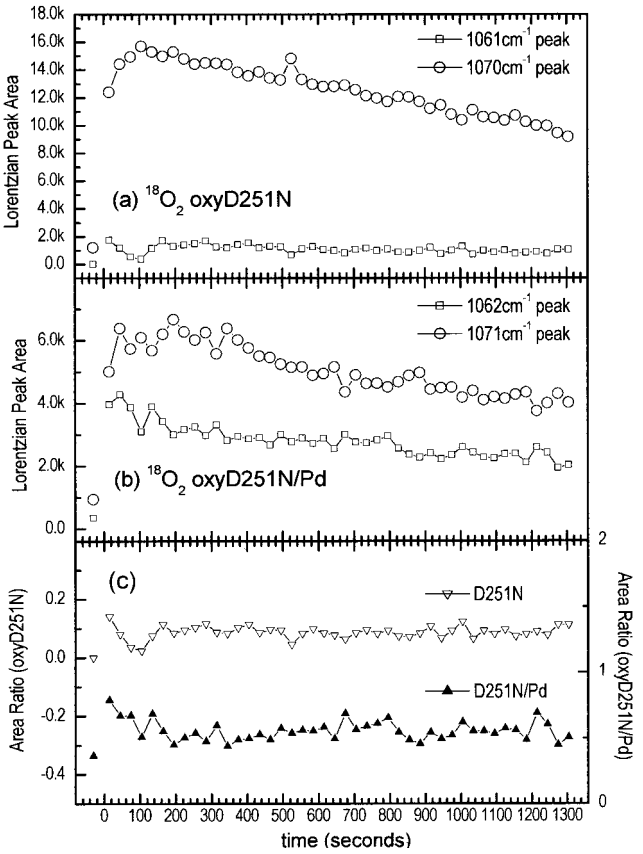

FIGURE 7: (a) Lorentzian peak area of the 1061 cm^{-1} (squares) and 1070 cm^{-1} (circles) peaks of D251N $^{18}O_2$- P450$_{cam}$. (b) Lorentzian peak area of the 1062 cm^{-1} (squares) and 1071 cm^{-1} (circles) peaks of D251N $^{18}O_2$-P450$_{cam}$/Pd complex. (c) Ratio of the Lorentzian peak area of the 1061 cm^{-1} peak to the 1070 cm^{-1} peak for D251N (upside down triangles) and D251N/Pd complex (filled triangles).

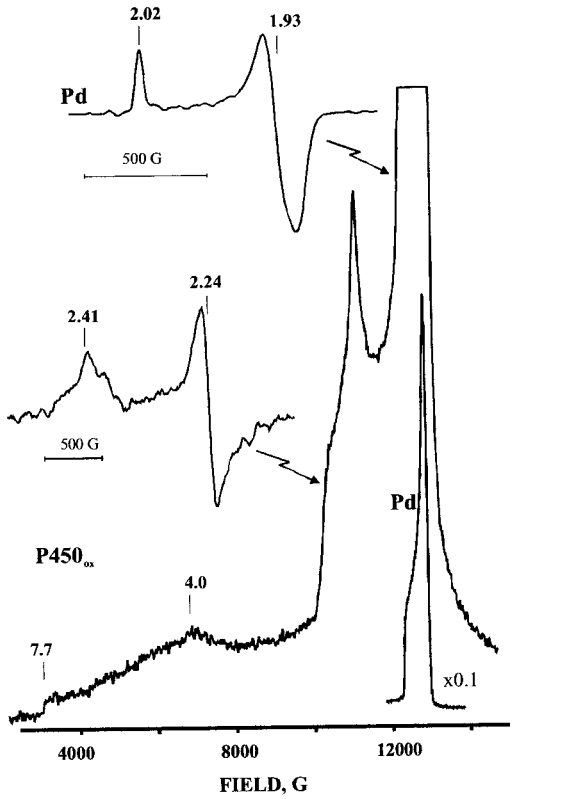

FIGURE 8: Q-band CW EPR spectra of the D251N oxy-P450$_{cam}$/Pd complex. The insets present an expanded view of the derivative EPR spectrum with the magnetic field scale shown as horizontal bars. The dominant signal comes from the Pd with *g*-values at 2.02 and 1.93. The minority signals from residual amounts of autoxidized P450$_{cam}$ (both high- and low-spin species) are also shown. There are no additional signals (*10*) attributable to the transfer of a second electron to the oxygen-bound ferrous heme.

identification of the intermediate involved in dioxygen activation. During enzymatic turnover, D251N P450$_{cam}$ shows a significantly red-shifted UV−visible absorption spectrum (both Soret and Q-band) compared to other catalytic intermediates (*23*, *24*). This intermediate (**5**) was tentatively identified as a reduced dioxygen bound intermediate with a peroxide electronic structure ($Fe^{3+}-O-O^{2-}$) (*23*) since the Soret band is often thought to be insensitive to structure, but very sensitive to electronic perturbations. Also, recent density functional theoretical calculations (*31*) of the optical spectrum of the reduced ferrous dioxygen model P450 **5** showed strong similarities to the optical spectrum of the new intermediate observed by Benson et al. (*23*). In the present paper, we use resonance Raman and EPR spectroscopy to characterize this intermediate more completely. We find that binding of reduced Pd to the oxygen complex of the D215N mutant perturbs the conformational substate populations of the O_2 species, but does not lead to an additional electron transfer from the Pd to the oxy-heme of P450$_{cam}$.

Figure 3 presents the high-frequency resonance Raman spectra of WT and D251N oxy-P450$_{cam}$. It should be noted that there are negligible differences in the "core size" marker band and dioxygen stretching (ν_{O-O}) frequencies, indicating that the D251N mutation does not affect the spin or coordination of the iron or the electronic structure of the oxygen. When we compare the RR spectrum of the D251N oxy-P450$_{cam}$/Pd complex to the uncomplexed D251N oxy-P450$_{cam}$, we see negligible differences in the "core size" marker bands, indicating that the iron atom remains in a "ferric like", low-spin, 6-coordinate state. This observation excludes the possibility that electron transfer to either the iron atom or the porphyrin ring has occurred upon binding of reduced Pd to the oxy complex. Moreover, Figures 5 and 6 show no large frequency shifts between D251N oxy-P450$_{cam}$ and the D251N oxy-P450$_{cam}$/Pd complex for the oxygen-sensitive modes at 540 cm^{-1} (ν_{Fe-OO}) and 402 cm^{-1} (δ_{Fe-O-O}). On the other hand, multiple components of the O_2 stretching mode (ν_{O-O}) do appear upon Pd complex formation, but the frequency of the major component remains the same as the uncomplexed material within, ±1 cm^{-1}.

These observations verify that in the D251N/Pd complex the dioxygen bond has not been severed and this intermediate is not an oxyferryl ($Fe^{4+}-O^{2-}$) species as observed by Schlichting et al. (*9*) following radiolytic reduction. Likewise, the lack of significant frequency changes in any of the oxygen vibrational modes suggests that the oxygen remains in a superoxide state ($Fe^{3+}-O-O^{-}$) very similar to the state of the WT and D251N oxy-P450$_{cam}$. If the D251N oxy-P450$_{cam}$/Pd intermediate was in a ferric peroxide state ($Fe^{3+}-O-O^{2-}$), as suggested by the experimental observations of Benson et al. (*23*) and by the theoretical calculations of Harris, Loew, and Waskell (*31*), it is expected that the frequencies associated with the bound dioxygen would be perturbed, which is not the case.

Very little information is available about the vibrational properties of iron−peroxide species due to their short lifetimes. Recently, the resonance Raman spectra of non-heme mononuclear low-spin iron−hydroperoxo (Fe^{3+}−OOH) and iron−peroxo (Fe^{3+}−OO) complexes have been observed (*32*, *33*). For the iron−hydroperoxo complex, the Fe−O mode was assigned at 620 cm^{-1} (*33*), and an oxygen stretching mode (ν_{O-O}) was assigned at 800 cm^{-1} (*33*) and 790 cm^{-1} (*32*). The frequencies for the peroxo complexes of the Fe−O and O−O stretching modes were 465 and 820 cm^{-1}, respectively (*33*). Therefore, the presence of ν_{O-O} near ∼1100 cm^{-1} indicates a superoxide rather than a peroxide or hydroperoxide oxidation state for the bound dioxygen. In further support of this claim, we present EPR data in Figure 8, which show no evidence for the peroxide state ($g = 2.25$, 2.16, 1.96) observed in the radiolytically reduced D251N oxy-$P450_{cam}$ or the hydroperoxide state ($g = 2.3$, 2.16, 1.96) observed for radiolytically reduced WT oxy-$P450_{cam}$ (*10*). The fact that there is no evidence of a second electron transfer from Pd to either the oxygen or the heme is consistent with the resonance Raman observations and indicates that the D251N mutation drastically reduces the rate of the second electron transfer from Pd to the dioxygen bound heme in $P450_{cam}$.

A previous study on the kinetic solvent isotope effect (KSIE) of $P450_{cam}$ has demonstrated that the rate of first proton transfer is significantly reduced in the D251N mutant (*34*). The turnover rates of the D251N mutant have a KSIE of 10 at pH 5.9 compared to 1.8 for WT at pH 7.0 (*34*) (KSIE = product formation rate in H_2O/product formation rate in D_2O). The rate of product formation and the KSIE have also been found to depend strongly on pH (*34*). For the D251N mutant, the rate of product formation decreases roughly 1 order of magnitude from pH 5 to 8. The current experiments were performed at pH 8 where the activity and KSIE are greatly reduced. It has been proposed (*34*) that D251 is a critical part of the normal proton delivery mechanism, and the D251N mutant disrupts normal proton delivery and also opens the O_2 binding site allowing for easier water access. The access of water to the active site explains both the large KSIE observed at low pH and the strong activity dependence on pH. The current experiment demonstrates that electron transfer is disrupted along with the proton-transfer mechanism in the D251N mutant. This suggests either that D251 is important in both electron and proton transfer or that the second electron transfer from Pd is dependent upon the proton transfer. One possibility is that electron and proton transfer involves a "dressed" state with a correlated motion between the positively and negatively charged particles.

The most profound Pd-induced effect in the resonance Raman spectrum of the D251N oxy-$P450_{cam}$ complex is the change in the conformational equilibrium of the bound dioxygen substates, which is clearly illustrated in Figure 4. Upon Pd binding, there is a large increase of a lower frequency conformational substate of the O_2 stretching mode near 1129 cm^{-1}. In earlier work on WT oxy-$P450_{cam}$ under catalytic conditions (*35*), there was no obvious perturbation of the O_2 stretching frequency. We propose that under catalytic conditions, the perturbation of the O_2 stretching frequency is negligible because the turnover to product is very fast and the population of this (active) intermediate conformation is very small. Since no differences are observed between the WT and D251N oxy-$P450_{cam}$ in the absence of Pd, we suggest that a similar change in the conformational substate distribution occurs upon Pd binding to WT oxy-$P450_{cam}$, and that the altered conformational distribution is related to the effector function of Pd.

Multiple O_2 stretching frequencies have also been observed when adamatanone is used as the substrate in WT oxy-$P450_{cam}$ (*8*). However, these conformational substates occurred in the absence of Pd and have higher O_2 stretching frequencies. The role of the substrate in altering the conformational substate population is not clear at this time, but given the need for close proximity between activated oxygen and substrate, it is not surprising to find that ν_{O-O} is substrate-specific.

The major spectroscopic effects of Pd binding to D251N oxy-$P450_{cam}$ are the red shift of the Soret and Q absorption bands [with a shift of 5 nm observed for both bands (*23*, *36*)], and the redistribution of the conformational substate population to favor a conformation with a 9 cm^{-1} downshift in ν_{O-O} and a 15 cm^{-1} downshift in ν_{Fe-OO}. As discussed earlier, the Raman marker bands and the EPR spectra demonstrate that electron transfer to the oxy-heme complex is not the origin of these perturbations.

Previous studies have shown that the heme active site of $P450_{cam}$ is perturbed upon Pd binding (*11*−*15*). For example, Unno et al. (*14*) observed a ∼3 cm^{-1} upshift in the Fe−S stretch frequency upon the binding of Pd to ferric $P450_{cam}$ while the Soret band exhibited a slight red shift. Makino et al. (*12*) and Unno et al. (*16*) observed an ∼8 cm^{-1} downshift in the C−O stretching frequency and an ∼3 cm^{-1} upshift in the Fe−CO stretching frequency upon binding of Pd to ferrous CO-$P450_{cam}$. Iron−diatomic ligand vibrations, such as ν_{Fe-XO}, and ν_{X-O}, where X = C, N, or O, have been extensively studied as sensitive structural probes of various heme proteins and model compounds. A negative linear correlation between ν_{Fe-XO} and ν_{X-O} is observed for both 5- and 6-coordinated Fe−XO porphyrins (*37*). The negative correlation is usually attributed to metal-to-ligand π back-bonding (*37*). In contrast, the conformational substates in the D251N oxy-$P450_{cam}$/Pd complex show a positive correlation between ν_{Fe-OO} and ν_{O-O}. This suggests that structural differences beyond simple π back-bonding must exist between the two conformational states. The red-shifted Soret and Q absorption bands provide evidence for a perturbation of the heme structural equilibrium since such shifts are potentially connected to nonplanar distortions of the porphyrin skeleton (*38*, *39*).

Another possible role of the conformational change associated with Pd binding is that it induces the thiolate ligand to compete more effectively with oxygen for the d_z^2 orbital of the iron atom. For example, Vogel et al. (*37*) have observed a positive correlation between ν_{Fe-OO} and ν_{O-O} in model thiolate complexes [e.g., see Table 2 of Vogel et al. (*37*)]. Such a situation would involve π back-donation, which weakens the O−O bond and strengthens the Fe−OO bond, but depending on the details of the thiolate hybridization state (sp^3, sp^2, etc.) (*40*), the sigma competition for the d_z^2 orbital might be strong enough to lead to an overall weakening of ν_{Fe-OO} along with ν_{O-O}.

The rich electronic structure associated with thiolate ligation to $P450_{cam}$ has been noted in previous work (*41*, *42*), where two separate blue-shifted S → Fe charge-transfer transitions have been observed underlying the Soret band of

the ferric enzyme. The data presented in Figure 2 demonstrate that complex electronic structure is also associated with the oxygenated complex. For example, note how the relative intensity of the δ_{FeOO} and ν_{Fe-OO} modes increases relative to the ν_{O-O} stretching mode as the laser is tuned to 356 nm. This indicates the presence of localized electronic excitations that have a differential effect on the iron-based vibrations (δ_{FeOO} and ν_{Fe-OO}) than on ν_{O-O}. The relative enhancement of δ_{FeOO} and ν_{Fe-OO} at 356 nm is reminiscent of the blue-shifted Raman excitation profiles observed for the Fe−S mode (*42*) and may be related to the unusual (positive) correlation between ν_{Fe-OO} and ν_{O-O} observed for the Fe−O_2 substates of P450$_{cam}$.

CONCLUSION

We have used resonance Raman spectroscopy to probe the effect of Pd binding to the D251N mutant of oxy-P450$_{cam}$. Previous work has proposed that this complex involved the reduction of the oxy-heme to a peroxy intermediate (*23*). However, we have determined that the D251N oxy-P450$_{cam}$/Pd complex is a low-spin, ferric-like, 6-coordinate complex with the dioxygen in a superoxo valence state. We find no evidence that transfer of the second electron from Pd to the oxy-heme has occurred in the D251N mutant. This indicates that the D251N mutation significantly retards the second electron transfer. This observation, along with the previously established fact that the proton transfer rate is greatly reduced in this mutant, suggests that the electron and proton transfer events may be coupled. We also observed that Pd binding significantly changes the conformational substate populations in the D251N mutant. The resonance Raman spectra and the red-shifted electronic spectra for the oxy-P450$_{cam}$/Pd complex suggest that Pd binding induces a structural perturbation of the oxy-heme. We propose that this structural perturbation is related to the effector function of Pd and may involve an alteration of the electron-donating properties of the thiolate ligand.

REFERENCES

1. Ortiz de Montellano, P. R. (1995) *Cytochrome P450 Structure, Mechanism, and Biochemistry*, Plenum Press, New York.
2. Gunsalus, I. C., Sligar, S. G., and Debrunner, P. G. (1975) *Biochem. Soc. Trans. 3*, 821−835.
3. Lipscomb, J. D., Sligar, S. G., Namtvedt, M. J., and Gunsalus, I. C. (1976) *J. Biol. Chem. 251*, 1116−1124.
4. Sligar, S. G., and Murry, R. I. (1986) in *Cytochrome P-450, Structure, Mechanism, and Biochemistry* (Ortiz de Montellano, P. R., Ed.) pp 429−503, Plenum Press, New York.
5. Sligar, S. G., Lipscomb, J. D., Debrunner, P. G., and Gunsalus, I. C. (1974) *Biochem. Biophys. Res. Commun. 61*, 290−296.
6. Brewer, C. B., and Peterson, J. A. (1986) *Arch. Biochem. Biophys. 249*, 515.
7. Bangcharoenpaurpong, O., Rizos, A. K., Champion, P. M., Jollie, D., and Sligar, S. G. (1986) *J. Biol. Chem. 261*, 8089−8092.
8. Hu, S. Z., Schneider, A. J., and Kincaid, J. R. (1991) *J. Am. Chem. Soc. 113*, 4815−4822.
9. Schlichting, I., Berendzen, J., Chu, K., Stock, A. M., Maves, S. A., Benson, D. E., Sweet, R. M., Ringe, D., Petsko, G. A., and Sligar, S. G. (2000) *Science 287*, 1615−1622.
10. Davydov, D., Macdonald, I. D. G., Makris, T. M., Sligar, S. G., and Hoffman, B. M. (1999) *J. Am. Chem. Soc. 121*, 10654−10655.
11. Lipscomb, J. D. (1980) *Biochemistry 19*, 3590−3599.
12. Makino, R., Iizuka, T., Ishimura, Y., Uno, T., Nishimura, K., and Tsuboi, M. (1984) in *Proceedings of the Ninth International Conference on Raman Spectroscopy*, pp 492−493, The Chemical Society of Japan, Tokyo.
13. Shiro, Y., Iizuka, T., Makino, R., Ishimura, Y., and Morishima, I. (1989) *J. Am. Chem. Soc. 111*, 7707−7711.
14. Unno, M., Christian, J. F., Benson, D. E., Gerber, N. C., Sligar, S. G., and Champion, P. M. (1997) *J. Am. Chem. Soc. 119*, 6614−6620.
15. Mouro, C., Bondon, A., Jung, C., Hui, B. H., De Certaines, J. D., Spencer, R. G., and Simonneaux, G. (1999) *FEBS Lett. 455*, 302−306.
16. Unno, M., Christian, J. F., Sjodin, T., Benson, D. E., Macdonald, I. D. G., Sligar, S. G., and Champion, P. M., unpublished experiments.
17. Stayton, P. S., and Sligar, S. G. (1990) *Biochemistry 29*, 7381−7386.
18. Koga, H., Sagara, Y., Yaoi, T., Tsujimura, M., Nakamura, K., Sekimizu, K., Makino, R., Shimada, H., Ishimura, Y., and Yura, K. (1993) *FEBS Lett. 331*, 109−113.
19. Nakamura, K., Horiuchi, T., Yasukochi, T., Sekimizu, K., Hara, T., and Sagara, Y. (1994) *Biochim. Biophys. Acta 1207*, 40−48.
20. Unno, M., Shimada, H., Toba, Y., Makino, R., and Ishimura, Y. (1996) *J. Biol. Chem. 271*, 17869−17874.
21. Pochapsky, T. C., Jain, N. U., Kuti, M., Lyons, T. A., and Heymont, J. (1999) *Biochemistry 38*, 4681−4690.
22. Pochapsky, T. C., Lyons, T. A., Kazanis, S., Arakaki, T., and Ratnaswamy, G. (1996) *Biochimie 78*, 723−733.
23. Benson, D. E., Suslick, K. S., and Sligar, S. G. (1997) *Biochemistry 36*, 5104−5107.
24. Gerber, N. C., and Sligar, S. G. (1992) *J. Am. Chem. Soc. 114*, 8742−8743.
25. Gunsalus, I. C., and Wagner, G. C. (1978) *Methods Enzymol. 52*, 166−188.
26. Werst, M. W., Davoust, C. E., and Hoffman, B. M. (1991) *J. Am. Chem. Soc. 113*, 1533−1538.
27. Macdonald, I. D. G., Sligar, S. G., Christian, J. F., Unno, M., and Champion, P. M. (1999) *J. Am. Chem. Soc. 121*, 376−380.
28. Shimada, H., Nagano, S., Ariga, Y., Unno, M., Egawa, T., Hishiki, T., Ishimura, Y., Masuya, F., Obata, T., and Hori, H. (1999) *J. Biol. Chem. 274*, 9363−9369.
29. Griffith, B. W., Peterson, J. A., and Eastabrook, R. W. (1979) in *The Porphyrins* (Dolphin, D., Ed.) pp 333−375, Academic Press, New York.
30. Shimada, H., Makino, R., Imai, M., Horiuchi, T., and Ishimura, Y. (1990) in *International Symposium on Oxygenase and Oxygen Activation* (Yamamoto, S., Nozaki, M., and Ishimura, Y., Eds.) pp 133−136, Yamada Science Foundation, Yamada, Japan.
31. Harris, D., Loew, G., and Waskell, L. (1998) *J. Am. Chem. Soc. 120*, 4308−4318.
32. Ho, R. Y. N., Roelfes, G., Feringa, B. L., and Que, L. (1999) *J. Am. Chem. Soc. 121*, 264−265.
33. Simaan, A. J., Dopner, S., Banse, F., Bourcier, S., Bouchoux, G., Boussac, A., Hildenbrandt, P., and Girerd, J.-J. (2000) *Eur. J. Inorg. Chem.* 1627−1633.
34. Vidakovic, M., Sligar, S. G., Li, H., and Poulos, T. L. (1998) *Biochemistry 37*, 9211−9219.
35. Egawa, T., Ogura, T., Makino, R., Ishimura, Y., and Kitagawa, T. (1991) *J. Biol. Chem. 266*, 10246−10248.
36. Gerber, N. C., and Sligar, S. G. (1994) *J. Biol. Chem. 269*, 4260−4266.
37. Vogel, K. M., Kozlowski, P. M., Zgierski, M. Z., and Spiro, T. G. (1999) *J. Am. Chem. Soc. 121*, 9915−9921.
38. Parusel, A. B. J., Wondimagegn, T., and Ghosh, A. (2000) *J. Am. Chem. Soc. 122*, 6371−6374.
39. Shelnutt, J. A., Song, X. Z., Ma, J. G., Jia, S. L., Jentzen, W., and Medforth, C. J. (1998) *Chem. Soc. Rev. 27*, 31−41.
40. Champion, P. M., Stallard, B. R., Wagner, G. C., and Gunsalus, I. C. (1982) *J. Am. Chem. Soc. 104*, 5469−5472.
41. Champion, P. M. (1989) *J. Am. Chem. Soc. 111*, 3433−3434.
42. Bancharoenpaurpong, O., and Champion, P. M. (1987) *J. Chem. Phys. 87*, 4273−4284.

BI002510B